Solid-fluid transition in a granular shear flow

Ashish V. Orpe and D. V. Khakhar*
Department of Chemical Engineering, Indian Institute of Technology - Bombay, Powai, Mumbai, 400076, India
(Dated: February 2, 2008)

The rheology of a granular shear flow is studied in a quasi-2d rotating cylinder. Measurements are carried out near the midpoint along the length of the surface flowing layer where the flow is steady and non-accelerating. Streakline photography and image analysis are used to obtain particle velocities and positions. Different particle sizes and rotational speeds are considered. We find a sharp transition in the apparent viscosity (η) variation with rms velocity (u). In the fluid-like region above the depth corresponding to the transition point (higher rms velocities) there is a rapid increase in viscosity with decreasing rms velocity. Below the transition depth we find $\eta \propto u^{-1.5}$ for all the different cases studied and the material approaches an amorphous solid-like state deep in the layer. The velocity distribution is Maxwellian above the transition point and a Poisson velocity distribution is obtained deep in the layer. The observed transition appears to be analogous to a glass transition.

PACS numbers: 45.70.-n, 45.70.Mg, 83.80.Fg

Granular materials are known to exist in solid-like and fluid-like states [1]. Physical understanding of the flow of granular materials has thus developed along two major themes based on the flow regime [2]. In the *rapid flow* — fluid-like — regime, both theory and experimental analysis are generally cast in the framework of the kinetic theory [3]. In contrast, the *slow flow* — solid-like — regime is most commonly described using the tools of soil mechanics and plasticity theory [4] and recently by analogy to glasses [5, 6, 7]. A key difference between solid-like and fluid-like states, which appears to be emerging from recent studies, is the definition of a temperature in the two states. In the fluid-like state the granular temperature is defined as the kinetic energy of velocity fluctuations in analogy with the kinetic theory of gases. In contrast, for dense granular flows (solid-like state), numerical [8] and experimental [9] studies show the validity of the fluctuation-dissipation theorem (the mean-square displacement of a particle is proportional to time for a constant applied force). This allows for the definition of a new temperature [7]. These two approaches have no well-understood region of overlap. Given the qualitative differences between the fluid and solid states, a question that has been open for some time relates to the criterion for transition between fluid and solid states of granular materials. We focus on this question.

There are few studies which focus on the transition between the solid and fluid states. Metcalfe et al. [10] studied solid to fluid transition in a horizontally vibrated container of beads. They observed hysteresis in the transition which was well-predicted by a dry friction model in which the friction coefficient varies smoothly between a dynamic and static value. A fluid-solid transition was also observed by D'Anna and Gremaud [5] for vertically vibrated particles. They found that the vibrating granular medium first undergoes a sharp transition to a supercooled liquid and then gradually achieves a solid-like state on reducing the intensity of vibration. This process follows a modified Vogel-Fulcher-Tammann (VFT) model which is typical of fragile glasses.

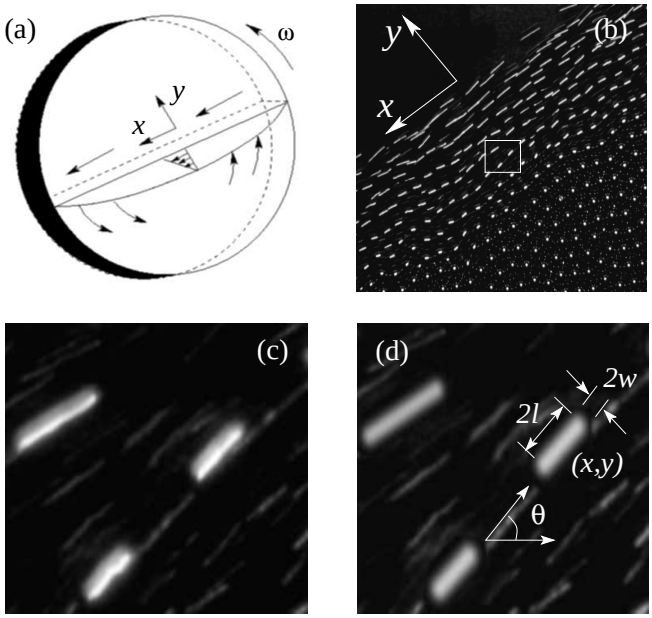

FIG. 1: (a) Schematic of the rotating cylinder geometry showing the flowing layer and the co-ordinate system employed. (b) A typical image showing the portion of the flowing layer at the center of the cylinder, with streaks of various lengths formed across the layer for a shutter speed of 1/250 s. (c) Magnified image of the rectangular region marked in (b) showing streaks generated by three different particles. (d) The same three streaks with the fitted intensity function. The optimization yields length ($2l$), width ($2w$), orientation angle (θ) and position (x, y) for every streak.

Coexisting solid and fluid phases have been studied primarily in the context of surface flows; these comprise

*Electronic address: khakhar@iitb.ac.in

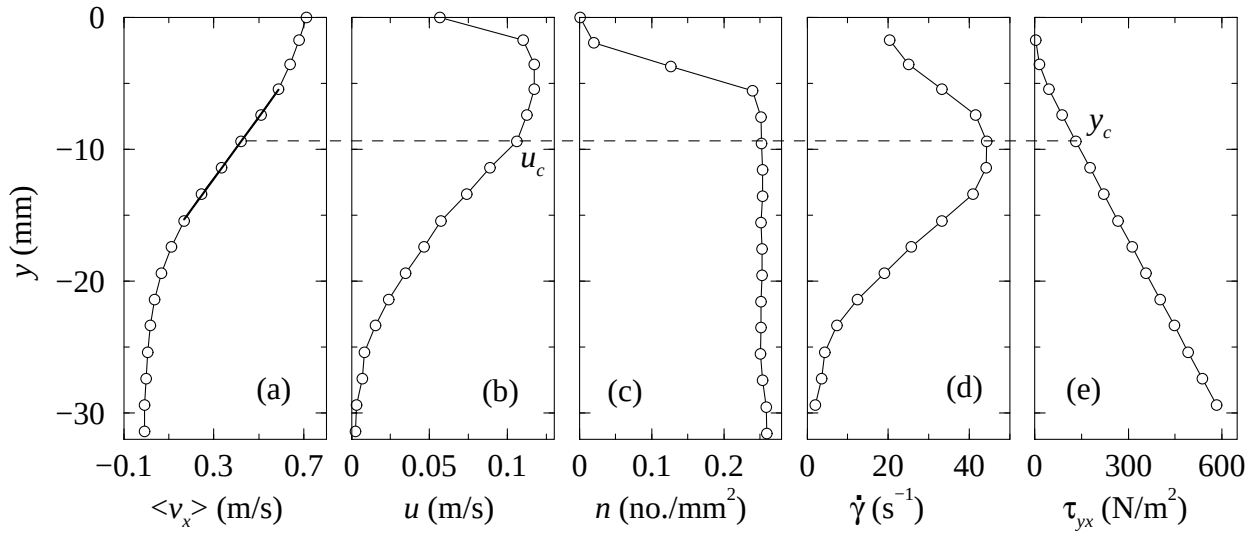

FIG. 2: Mean velocity ($\langle v_x \rangle$), rms velocity (u), number density (n), shear rate ($\dot{\gamma}$) and shear stress (τ_{yx}) across the flowing layer for 2 mm steel balls rotated at 3 rpm. The solid line in (a) shows a linear fit to the mean velocity profile. The dashed line denotes the transition point in all the figures.

a layer of fluid like flow on a fixed bed of the same material. Examples of surface flows which have been well-studied include heap flows [11, 12, 13, 14, 15, 16, 17] and rotating cylinder flows [18, 19, 20, 21, 22, 23, 24]. Remarkably simple theories describe the coexistence between the solid and fluid. In the simplest versions, the local *melting* and *freezing* is determined by the local angle of the solid-fluid interface: If the local angle is greater than a "neutral" angle, the solid melts (the heap erodes) so as to reduce the angle and vice versa [11, 12]. Continuum models based on Coulombic friction models for the solid region and simple rheological models for fluid region predict a similar behaviour [14, 17]. Experimental studies show that the models based on local angle based melting/freezing give good predictions [17].

An assumption in the coarse-grained models described above is the existence of an interface between the solid and fluid. However, the recent work of Komatsu et al. [15] indicates that the surface flow on a heap decays smoothly with depth and generates motion deep within the heap. The interface between the solid and fluid regions is thus not well-defined when considered at a particle length scale. Studies of the velocity profile in rotating cylinders flow also confirm this picture of a smooth decay of the velocity into the bed, rather than an abrupt change at an interface [22, 23].

The objective of the present work is to gain an insight into the fluid-solid transition in granular flows focussing on a system where both fluid-like and solid-like regions coexist. We find a well-defined transition point in the system which demarcates two distinct flow regions. The behaviour in each region is characterized and results indicate that the transition has some characteristics of a glass transition.

Experiments are carried out in quasi-2d aluminium cylinders (length 1 or 2 cm) of radius 16 cm (Fig. 1a). The end walls are made of glass and a computer controlled stepper motor with a sufficiently small step is used to rotate the cylinders. Monodisperse, spherical, shiny stainless steel balls of three different sizes with diameters (d) 1, 2, and 3 mm are used in the experiments. Cylinder rotation in the rolling flow regime (rotational speed, $\omega = 2 - 9$ rpm) produces a thin flowing surface layer and measurements are made near the center of the cylinder where the layer thickness is maximum and the flow is non-accelerating. The particles are heavy enough and conductive so that charge effects are negligible. The experiments are carried out with 50% of the cylinder filled with particles.

The motion of the particles is captured by taking high resolution images using a digital camera (Nikon Coolpix 5000) in the presence of an incident beam of light. The size of the recorded region is 2560×1920 pixels, with one pixel corresponding to $0.016 - 0.03$ mm depending on the distance of the camera to the cylinder. The point source of light is directed near parallel to the end wall of the cylinder so as to illuminate only the front layer of the flowing particles. Each moving particle generates a streak of definite length depending on its speed and the shutter speed of the camera. Images are taken for a range of camera shutter speeds ($1/15 - 1/2000$ s) so as to account for the varying velocity across the flowing layer. This gives streaks, which are adequately long for analysis but not so long as to overlap with other streaks, in each the part of the flowing layer (Fig. 1b). Two hundred images are taken for each shutter speed with an overall of two thousand images combined over different shutter speeds. Due to the time interval between photographs, each experiment typically takes 500 cylinder revolutions.

A parameterized intensity function corresponding to a

stretched Gaussian function is then fitted to the intensity values of the streak pixels (and an immediate neighbourhood) in the image by means of a standard non-linear optimization technique. The fitting yields the length ($2l$), width ($2w$), orientation angle (θ) and the position (x, y) for the streak (Fig. 1d). The analysis technique was calibrated by carrying out experiments for a single particle glued to the cylinder end plate. The error in velocity measurements was found to be less than than 3%. For analysis, the flowing layer region is divided into bins of width equal to the particle diameter and length 20 mm parallel to the flowing layer. The components of the mean and the root mean square (rms) velocities for each bin are calculated by averaging over all streaks in a bin.

Fig. 2 gives the variation of system variables with depth (y) in the flowing layer for 2 mm particles. The mean velocity ($\langle v_x \rangle$) profile is smooth and shows 3 regions; a near-linear middle region, an exponentially decaying region at the bottom and a flattened region near the top. Similar profiles have been reported in several previous studies [22, 23, 24, 25, 26, 27, 28, 29]. The flattened upper region which is the very low density region corresponding to saltating particles is not seen in some studies. The magnitudes of the rms velocities in the two directions are different: the component in the flow direction (x-component) is about 10% higher than that in direction perpendicular to the flow (y-component). The profile of the total magnitude of the fluctuating velocities (u) is shown in Fig. 2b. The rms velocity profile shows two distinct regions: a relatively slow variation near the free surface followed by a sharper decrease deeper in the bed. Fig. 2d shows the shear rate variation in the layer, obtained by numerical differentiation of the data in Fig. 2a. The shear rate increases to a maximum value (corresponding to the inflection point in the velocity field) and then decreases. We note that an oscillating shear rate profile is obtained if a smaller bin size is used as reported previously [24, 27, 29]. The transition point in the fluctuation velocity profile coincides with the maximum in the shear rate. The areal number density is almost constant throughout the flowing layer with a rapid decrease near the free surface as shown in Fig. 2c.

For non-accelerating flows a force balance yields the shear stress as $d\tau_{xy}/dy = \rho g \sin\beta \approx \rho_b (n/n_b) g \sin\beta$ where g is acceleration due to gravity, β is the angle of repose, n is the number density in the flowing layer, n_b is the number density in the rotating packed bed and ρ_b is the bulk density of the rotating packed bed. We neglect the contribution of wall friction in the estimate. This could become significant deeper in the bed [28]. However, based on the method of Taberlet et al. [28] we find that the contribution is about 10% of the total stress in the cases studied and does not qualitatively affect the results. Upon integration we obtain $\tau_{xy} = (\rho_b/n_b) g \sin\beta \int_y^0 n dy$ assuming $\tau_{xy} = 0$ at the free surface. The shear stress shows a near linear increase with depth (Fig. 2d). The results of Fig. 2 indicate that there is a qualitative change in the rheology at the transition point (y_c). Above y_c, the shear stress increases with shear rate which is typical of fluids. However, below y_c the shear stress increases while the shear rate decreases. This implies that the viscosity increases sharply with depth below y_c, even though the number density is nearly constant.

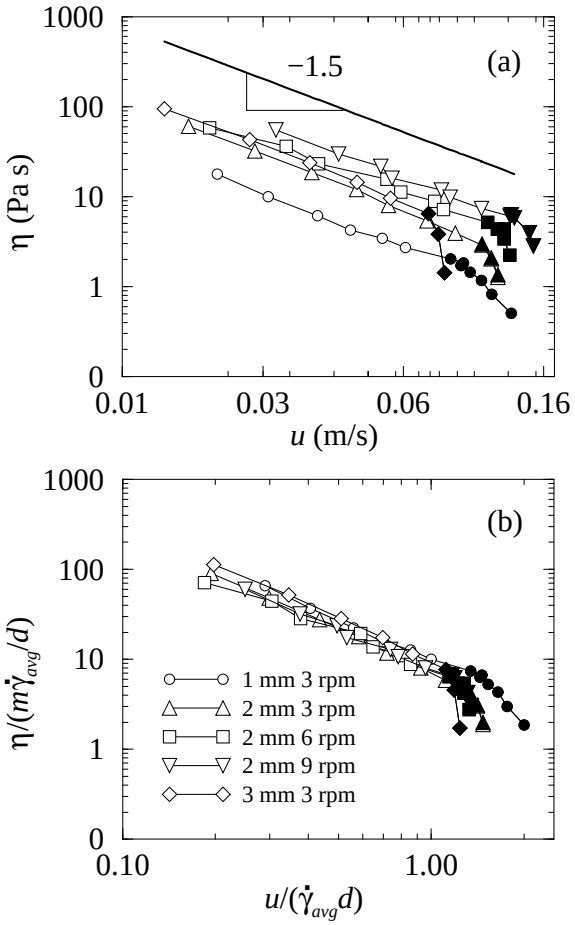

FIG. 3: Apparent viscosity (η) variation with rms velocity (u) for all the cases studied. Filled symbols represent the points at and above the transition velocity (u_c). (a) The solid line at the top represents a linear fit (slope $\simeq 1.5$) to the data below the transition point for all the cases studied. (b) The data is scaled using particle mass (m), particle diameter (d) and average shear rate obtained by a linear fit to each corresponding velocity profile.

Fig. 3a shows the variation of the apparent viscosity ($\eta = \tau_{xy}/\dot{\gamma}$) with the rms velocity (u), considering only the region of constant density. The data points at and above the transition point ($y \geq y_c$) are plotted as filled symbols. There is a sharp transition in this case as well and the transition occurs at the same value of u as in Fig. 2b. In the region near the free surface there is a rapid increase in viscosity with decreasing rms velocity whereas in the region approaching the fixed bed there is a much slower power law increase with an exponent $n \sim -1.5$ for all the cases studied. The data scales with $\dot{\gamma}_{avg}$ and d to fall on a single curve (Fig. 3b), and the

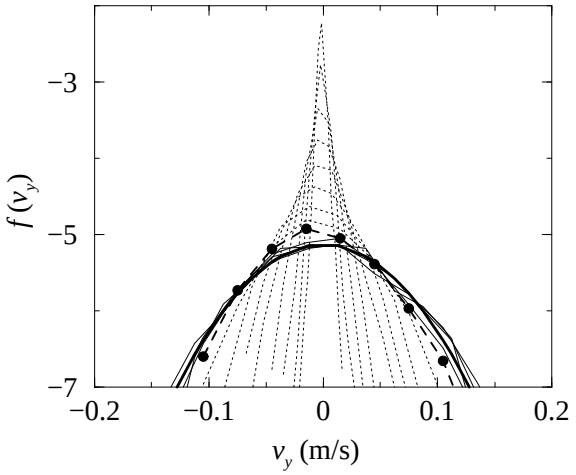

FIG. 4: Distributions of velocity in y direction at various locations across the layer for 2 mm steel balls rotated at 3 rpm. The dashed line with filled circles represents the transition point, the solid lines represent the region above the transition point and all the dotted lines represent the region below the transition point. The thick black line represents a fitted parabola to the curves at and above the transition point.

transition occurs at $u_c \sim 1.2\dot{\gamma}_{avg}d$ for all cases. Here $\dot{\gamma}_{avg}$ is the shear rate obtained by fitting a straight line to the linear portion of the velocity profile (Fig. 2a).

Fig. 4 shows the distributions of the y direction velocities at different locations in the layer. The v_y distribution is Gaussian for all points above the transition point ($y \geq y_c$) and it gradually evolves to a Poisson distribution as we go deeper into the bed. A Poisson velocity distribution was also found by Mueth [27] for Couette flow of a dense granular material. The v_x distribution (not shown) is Gaussian above the transition point. However, below the transition point the behaviour is complex and bimodal distributions are obtained.

The results presented show a sharp transition between two flow regimes. In the upper region near the free surface, the behaviour is fluid-like and the velocity distributions are Maxwellian. Below the transition point the material appears to be an amorphous soft solid, increasing in strength with depth in the layer. The transition to this solid-like regime occurs at a relatively large rms velocity (≈ 0.1 m/s). We conjecture that the sharp transition occurs because of the formation of a percolated network of particles in extended contact with each other. This is in contrast to the fluid-like regime where the particles interact through collisions. The contact network coexists with fluid-like domains and the fraction of particles which are part of the network increase with depth. The transition appears to be analogous to a glass transition. New rheological models may be required for granular flows that span these two regimes.

[1] H. M. Jaeger, S. R. Nagel, and R. P. Behringer, Rev. Mod. Phys. **68**, 1259 (1996).
[2] R. Jackson, J. Rheol. **30**, 907 (1986).
[3] C. S. Campbell, Annu. Rev. Fluid Mech. **22**, 57 (1990).
[4] R. M. Nedderman, *Statics and Kinematics of Granular Materials* (Cambridge Univ. Press, Cambridge, 1992).
[5] G. D'Anna and G. Gremaud, Nature **413**, 407 (2001).
[6] A. Barrat, J. Kurchan, V. Loreto, and M. Sellitto, Phys. Rev. E **63**, 051301 (2001).
[7] J. Kurchan, J. Phys. Condens. Matter **12**, 6611 (2000).
[8] H. A. Makse and J. Kurchan, Nature **415**, 614 (2002).
[9] G. D, Anna, P. Mayor, A. Barrat, V. Loreto, and F. Nori, Nature **424**, 909 (2003).
[10] G. Metcalfe, S. G. K. Tennakoon, L. Kondic, D. G. Schaeffer, and R. P. Behringer, Phys. Rev. E **65**, 031302 (2002).
[11] J. P. Bouchaud, M. Cates, J. Ravi Prakash, and S. F. Edwards, J. Phys. Paris I **4**, 1383 (1994).
[12] T. Boutreux, E. Raphaël, and P. G. de Gennes, Phys. Rev. E **58**, 4692 (1998).
[13] Y. Grasselli and H. J. Herrmann, Eur. Phys. J. B **10**, 673 (1999).
[14] S. Douady, B. Andreotti, and A. Daerr, Eur. Phys. J. B **11**, 131 (1999).
[15] T. S. Komatsu, S. Inagaki, N. Nakagawa, and S. Nasuno, Phys. Rev. Lett. **86**, 1757 (2000).
[16] P. A. Lemieux and D. J. Durian, Phys. Rev. Lett. **85**, 4273 (2000).
[17] D. V. Khakhar, A. V. Orpe, P. Andresén, and J. M. Ottino, J. Fluid Mech. **441**, 255 (2001).
[18] J. Rajchenbach, Phys. Rev. Lett. **65**, 2221 (1990).
[19] T. Elperin and A. Vikhansky, Europhys. Lett. **42**, 619 (1998).
[20] A. V. Orpe and D. V. Khakhar, Phys. Rev. E **64**, 031302 (2001).
[21] D. V. Khakhar, A. V. Orpe, and J. M. Ottino, Adv. Complex Systems **4**, 407 (2001).
[22] N. Jain, J. M. Ottino, and R. M. Lueptow, Phys. Fluids **14**, 572 (2002).
[23] D. Bonamy, F. Daviaud, and L. Laurent, Phys. Fluids **14**, 1666 (2002).
[24] K. M. Hill, G. Gioia, and V. V. Tota, Phys. Rev. Lett. **91**, 064302 (2003).
[25] L. Bocquet, W. Losert, D. Schalk, T. C. Lubensky, and J. P. Gollub, Phys. Rev. E **65**, 011307 (2001).
[26] S. Longo and A. Lamberti, Exp. Fluids **32**, 313 (2002).
[27] D. M. Mueth, Phys. Rev. E **67**, 011304 (2003).
[28] N. Taberlet, P. Richard, A. Valance, W. Losert, J. M. Pasini, J. T. Jenkins, and R. Delannay, Phys. Rev. Lett. **91**, 264301 (2004).
[29] D. M. Mueth, G. F. Debregeas, G. S. Karczmar, P. J. Eng, S. R. Nagel, and H. M. Jaeger, Nature **406**, 385 (2000).